Electron Paramagnetic Resonance Imaging of the Spatial Distribution of Free Radicals in PMR-15 Polyimide Resins

Myong K. Ahn*

Department of Chemistry, Indiana State University, Terre Haute, Indiana 47809

Sandra S. Eaton and Gareth R. Eaton

Department of Chemistry and Biochemistry, University of Denver, Denver, Colorado 80208

Mary Ann B. Meador

NASA Lewis Research Center, Cleveland, Ohio 44135

Received April 28, 1997; Revised Manuscript Received September 19, 1997[⊗]

ABSTRACT: Prior studies have shown that free radicals generated by heating polyimides above 300 °C are stable at room temperature and are involved in thermo-oxidative degradation in the presence of oxygen gas. Electron paramagnetic resonance imaging (EPRI) is a technique to determine the spatial distribution of free radicals. X-band (9.5 GHz) EPR images of PMR-15 polyimide were obtained with a spatial resolution of ∼0.18 mm along a 2-mm dimension of the sample. In a polyimide sample that was not thermocycled, the radical distribution was uniform along the 2-mm dimension of the sample. For a polyimide sample that was exposed to thermocycling in air for 300 1-h cycles at 335 °C, one-dimensional EPRI showed a higher concentration of free radicals in the surface layers than in the bulk sample. A spectral-spatial two-dimensional image showed that the EPR lineshape of the surface layer remained the same as that of the bulk. These EPRI results suggest that the thermo-oxidative degradation of PMR-15 resin involves free radicals present in the oxygen-rich surface layer.

Introduction

Polyimides are high-performance polymers that are used as matrix materials in fiber-reinforced composites for high temperature applications. Such composites, because of their light weight, relatively high strength, and high use temperatures (>300 °C), are finding increasing use in the electronics and aerospace industries.[1,2]

Thermally generated free radicals are found in polyimides that have been exposed to temperatures ≥ 300 °C.[3] These free radicals are stable at room temperature and are involved in oxidative degradation of polyimides in the presence of oxygen gas.[4] Electron paramagnetic resonance (EPR) spectroscopy is a technique for detecting unpaired electron spins in free radicals.[5,6] Electron paramagnetic resonance imaging (EPRI) provides the spatial distribution of these free radicals.[7] In this paper we report the room temperature spatial distributions of free radicals in PMR-15 polyimide resins as detected by EPRI using a magnetic field gradient to encode the spatial information.[8]

Experimental Section

Two PMR-15 samples, *a* and *b*, were prepared at the NASA Lewis Research Center following a standard two-stage synthetic method.[9] Details of the procedures for sample preparation and postcuring (PC) were published previously.[10] Neat resin plates were compression-molded from an imidized powder at 315 °C and pressures of 240−500 psi. After molding sample *a*, PC was carried out at 315 °C for 16 h in a nitrogen gas atmosphere. The sample was then subjected to an automated thermocycling process.[11] The sample was suspended from a pneumatically actuated disc above an alumina tube furnace, which was held at 335 °C with flowing air. The sample was lowered into the furnace for 1 h. Then, the sample was pneumatically removed from the furnace and held until it reached room temperature (∼10 min). This process of heating and cooling was repeated for 300 cycles. Physical changes associated with the thermocycling of sample *a* were examined with optical microscopy as reported previously for similar samples.[10,11]

Sample *b* was cut from a larger square piece prepared earlier for X-band EPR signal intensity studies.[5] This sample was pressure molded, and postcured at 316 °C in air for 16 h and then at 371 °C in nitrogen gas atmosphere for 30 h. These curing sequences are known[3] to produce large concentrations of free radicals in PMR-15.

EPR spectra were obtained with 0.08 mW microwave power, 1 gauss (G) modulation amplitude, and 50-G scans on a Varian E9 EPR spectrometer. (1 G = 0.1 mT). Figure 1 shows the first-derivative EPR spectra of the two PMR-15 samples (*a* and *b*). Figure 2 shows photographs of these samples. The sample dimensions and EPR characteristics are listed in Table 1. The signal intensity listed in Table 1 is the double-integral in arbitrary units divided by the mass of the sample. No attempt was made to correct for the nonuniformity of microwave magnetic field strength in the EPR cavity, which should introduce a relatively small correction in relative values for such similar samples. The data show that the unpaired spin concentration in sample *b* was ∼3.4 times that in *a*. Because sample *b* was treated at higher temperature (371 °C) than sample *a* (335 °C), this difference is consistent with increasing average radical production at higher PC temperature.

Comparison of the EPR spectra of the two samples shows, within experimental error, the same line position with a *g* value of 2.003[12] and similar lineshapes with a peak-to-peak linewidth (Δw_{pp}) of 5.5 G. These spectral similarities suggest that the free radicals in *a* and *b* have similar molecular structure, and that the nature of the room-temperature-stable free radicals in PMR-15 is not strongly dependent on the presence or absence of oxygen during heating or on the temperature at which the sample was heated. The symmetric absorption lineshape and the Δw_{pp} value of 5.5 G indicate that hyperfine coupling constants, anisotropic dipolar interactions, and the orientation dependence of resonance due to *g* anisotropy are less than a few gauss ($\Delta w_{pp}/2$).

The EPR signal intensity (Table 1) reflects the average radical concentrations in the samples. To examine the spatial distribution of radicals, EPRI was performed. The EPRI experiments were carried out as described previously.[8] A set

[⊗] Abstract published in *Advance ACS Abstracts,* December 15, 1997.

S0024-9297(97)00580-9 CCC: $14.00 © 1997 American Chemical Society

Table 1. EPR Imaging Samples

sample	mass, g	relative intensity	imaging dimension, mm	approximate other dimensions and shapes	thermocycling
a	0.1848	1.0	2.2	10 × 7 mm rectangular	300 cycles at 330 °C in air
b	0.1426	3.4	2.2	10 × 9 mm irregular diamond diagonals	none

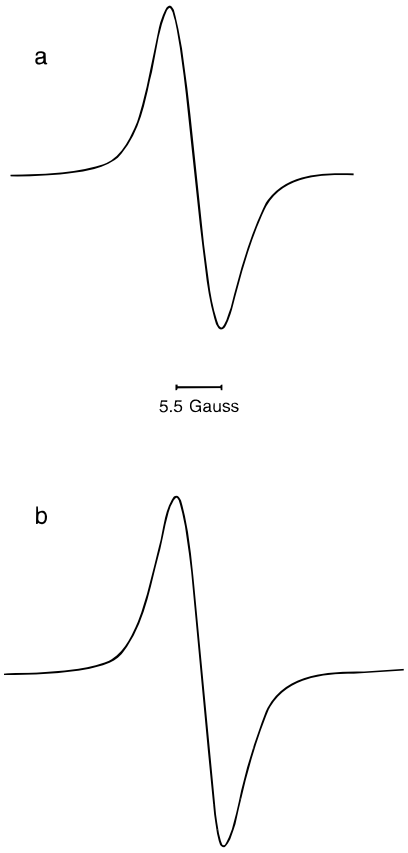

Figure 1. X-band EPR first-derivative spectra of PMR-15 imaging samples. Sample *a* (Figure 1a) was thermocycled in air for 300 cycles at 335 °C, and sample *b* (Figure 1b) was not thermocyled. The derivative peak-to-peak width is 5.5 G, and the relative intensities are listed in Table 1.

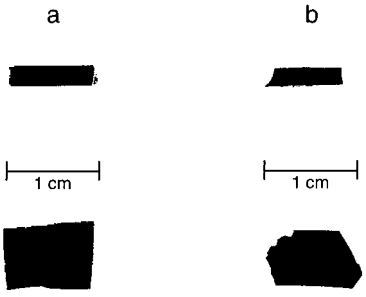

Figure 2. Photographs of PMR-15 EPR imaging samples *a* and *b*. The dimensions and sample specifications are listed in Table 1. The 2-mm dimension that was oriented along the applied magnetic field gradient is shown above the ruler. The perpendicular face is shown below the ruler. In a 1D image, the spin density is integrated over the cross-sectional area. Note that in sample *b*, the cross-sectional area varies along the 2-mm dimension and this is reflected in the image intensity as a function of the imaging dimension in Figure 3b.

of Helmholtz coils provided a maximum magnetic-field gradient of 300 G/cm along the direction of the main applied magnetic field. For each of the samples, we obtained one-dimensional (1D) spatial images with the gradient along the ~2 mm dimension of the sample, as shown in Figure 2. For this field gradient and Δw_{pp} of 5.5 G, the resolution of the 1D images is ~0.18 mm [i.e., 5.5 G/(300 G/cm)] unless the EPR lineshape is deconvoluted as discussed in the following section.

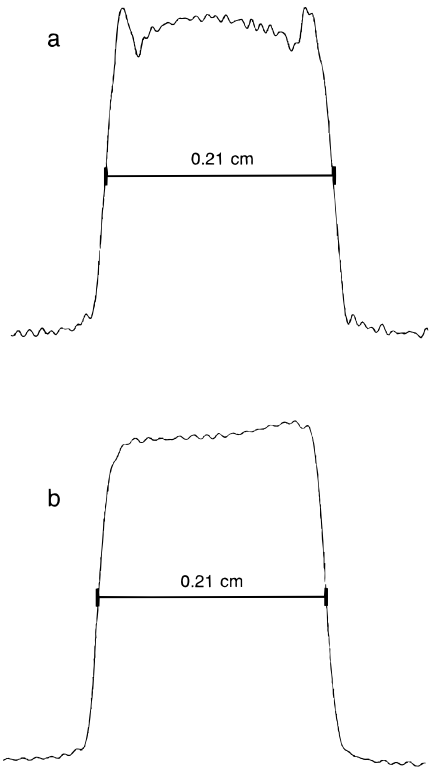

Figure 3. One-dimensional EPR images of PMR-15 samples *a* and *b* described in Table 1. Imaging is carried out with a 300 G/cm gradient applied in the direction of the 2-mm sample dimension. The resolution is improved by deconvolution of the EPR lineshape observed in the absence of the applied magnetic field gradient. The gradual rise of the EPR signal intensity from left to right in the image for sample *b* is caused by the irregular cross-sectional area along the 2-mm dimension.

The alignment of the sample relative to the gradient is another factor that impacts the resolution of the 1D images. Samples were supported on a quartz rod with a vertical flat region. Rotation around the long axis of the rod was adjusted to make the edge of the spatial profile as sharp as possible. Based on changes that we could detect in the image as a function of rotation, the error in alignment is <2° and probably closer to 1°. For an object with a horizontal dimension perpendicular to the applied field gradient of ~7 mm, this alignment error causes a broadening of the spatial profile of 0.24 mm if the error is 2° or of 0.12 mm for 1°, which is of the same order as the resolution estimated from the signal linewidth and the magnitude of the gradient. The 1D images that are shown in Figure 3 are of samples that were considered to be well oriented. The apparent thickness of each plate obtained from the images was in good agreement with values obtained using calipers to measure the sample, which confirms that the samples were reasonably well aligned.

In the presence of the magnetic field gradient, the EPR signal spreads out along the applied magnetic field direction. If the signal is weak, the maximum gradient may be limited by the need for acceptable signal-to-noise, which would limit the resolution of the image. However, for samples *a* and *b*, the EPR signal was strong enough that resolution was not limited by the signal-to-noise ratio.

Results

As discussed in the preceding section, the spatial resolution of the 1D images is estimated to be ~0.18

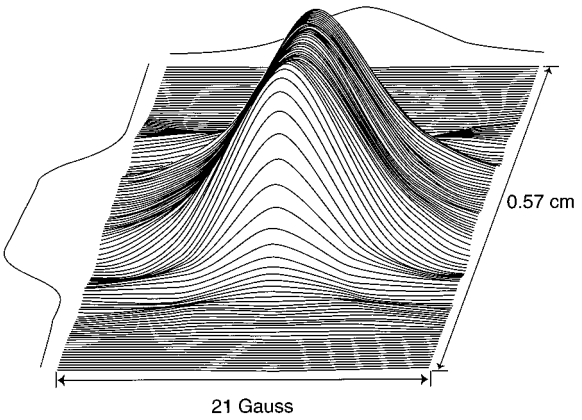

Figure 4. A 2D spectral−spatial EPR image of sample *a* shows a uniform lineshape along the 2-mm dimension. Reconstruction from an incomplete set of projections produces "missing angle ridges" that extend out from sharp boundaries.[8] These artifacts, present on the left and right sides of the image in the figure, degrade the resolution of the spatial projection shown to the left of the image and cause some distortion in the wings of the spectral slices near the front and back surfaces of the sample.

mm along the 2-mm dimension of the sample. The symmetric EPR lineshape indicates no significant complications due to anisotropic magnetic interactions of the unpaired electrons. The resolution of the 1D images was enhanced by deconvolution of the EPR lineshape. This deconvoluting was done by dividing the Fourier transform of the data in the presence of the gradient by the Fourier transform of data in the absence of gradient. Deconvoluted 1D images of *a* and *b* along the 2-mm sample dimension are shown in Figure 3. The minor oscillations were introduced by the deconvolution process. For sample *a*, the 1D image clearly shows that there was a higher radical concentration on the surface than in the bulk sample. This difference is enhanced by deconvolution with a nongradient spectrum. By contrast, we found no evidence of significant spatial variation in radical concentration in sample *b*. The slight variations for *b* probably are the result of the irregular edges of this sample.

Figure 4 shows a two dimensional (2D) spectral−spatial image of *a* using a maximum gradient of 300 G/cm, 60 experimental and four missing projections,[8] and reconstruction on a 128 × 128 grid. The resolution of a spatial slice through the 2D image is similar to that of the 1D image before deconvolution. This 2D image shows that the EPR lineshape remains approximately the same along the spatial dimension. Thus, the significant variation in the peak intensity along the spatial direction of the 1D image is due to variations in the unpaired electron spin densities (i.e., the free radical concentration). The 2D image also shows that the EPR signal height has maxima at the edges of the sample and is approximately constant in the middle of the sample, which is in agreement with the 1D image. Thus, the EPRI experiments show that oxygen caused a higher radical concentration on the surface of the sample.

Discussion

PMR-15 is the most widely studied polyimide resin material. Its long-term thermo-oxidative stability has been studied for the past 20 years. Our earlier studies showed that free radicals are present at room temperature in polyimides.[3,4] These free radicals are thermally generated during curing or aging processes at temperatures >300 °C. The free radicals remain stable at room temperature and can be detected by EPR. Comparisons of weight loss data with the free radical concentrations established that these free radicals are involved in the long-term thermo-oxidative degradation of the material in the presence of oxygen gas. In the absence of oxygen gas exposure, the PMR-15 resin samples that were aged at temperatures up to 370 °C retain mass within 5% of the initial value over 2000 h of testing, however, room-temperature-stable free radicals are generated and their concentration reaches a steady state value after ∼400 h.[5]

For an amorphous solid sample containing low concentrations of free radicals with nearly isotropic magnetic parameters, Δw_{pp} is determined by unresolved hyperfine interactions of the electron spin with nuclear spins in the free radical moiety. The hyperfine coupling constant, A_n, is directly proportional to the probability of finding the unpaired electron at nucleus n. For aromatic organic radicals, hyperfine interactions are predominantly with protons that have nuclear spin $I = 1/2$ and with ^{14}N that has $I = 1$. When the unpaired electron is in a conjugated π molecular orbital consisting of aromatic carbons or hetero atoms, the McConnell equation[13,14] (eq 1) predicts the ^1H hyperfine coupling constant, A_H:

$$A_H = Q\rho \tag{1}$$

where Q is 25 + 5 G for carbon, and ρ is the unpaired π-electron density at the aromatic carbon nucleus to which the H atom is bonded. The observed 5.5 G linewidth for the radicals in samples *a* and *b* is considerably smaller than the value of 25 G predicted by eq 1 for $\rho = 1$, which means that the spin density is not localized on a single carbon. Instead, the unpaired electron is delocalized over a large number of aromatic atoms. This conclusion is consistent with ENDOR[15] and high-field EPR studies of polyimides.[12] The room temperature stability of the free radicals detected by EPR results from the extensive delocalization of the unpaired electrons.

The EPR images (Figures 3a and 4) of sample *a*, which had been treated by thermocycling at 335 °C in the presence of oxygen gas, show that the concentration of free radicals is higher in the 0.1−0.2-mm thick surface layers than in the bulk material. The EPR image (Figure 3b) of sample *b*, which has not been subject to thermocycling, shows that the spatial distribution of free radicals is relatively uniform across the sample.

Bowles, Jayne, and Leonhardt[10] reported, based on microscopic examinations, that oxidative degradation of polyimide proceeds with development of cracks on the surface layer of the cured resin. Meador, Lowell, Cavano, and Herrera-Fierro[11] subsequently studied the surface reaction layer with Fourier transform-infrared (FT-IR) and scanning electron microscopy/electron density screening (SEM/EDS) techniques and found the layer to be rich in oxygen. They also reported that crack formation in neat resins is highly dependent on aging time and temperature but not on thermocycling frequency. We also note that there are at least two different types of cracking modes for composites, they are, surface cracking caused by oxidation that is not related to thermocycling, and interface or interlaminar cracking that is related to thermocycling.[10] During the aging process in oxygen atmosphere at elevated tem-

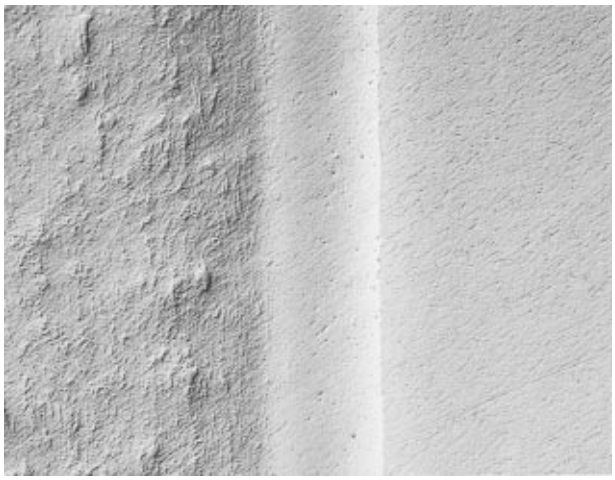

Figure 5. 200× microscopic image of sample *a*. The bulk of the PMR-15 sample is shown on the left side adjacent to the 0.2 mm smooth surface layer in the mid-vertical section. The remainder of the smooth region to the right of the surface layer is the epoxy resin used to mount the sample. The surface layer is found to be richer in oxygen than the sample bulk.

peratures, the sample mass and size decreased as a result of oxidative degradation, but the thickness of the surface reaction layer remained ~0.1−0.2 mm. A microscopic photograph of sample *a* (Figure 5) shows the 0.1-mm thick oxygen-rich surface layer. The thickness of this layer compares well with the thickness of the free-radical-rich layer found by EPRI in this work.

The possible involvement of free radicals in the crosslinking process or during curing of PMR-15 has been suggested previously.[16] A recent ^{13}C NMR study[17] of isotopically enriched PMR-15 strongly suggests that the reactive norbornene endcap undergoes crosslinking through a biradical intermediate.[17] Additional NMR evidence[18] indicated that the methylene group in the methylene dianiline (MDA) fragment of PMR-15 was converted to a carbonyl group through free radical intermediates in the elevated temperature oxidative degradation environment. The alkyl linkages of the endcaps are expected to be among the weakest chemical bonds, so these may cleave homolytically to produce diradicals. However, the EPR lineshapes and *g* values of the free radicals in polyimides such as AVIMID-N[5,19] that contain no norbornene endcaps or differently bonded linkages are indistinguishable from the EPR spectra of the radicals in PMR-15. This similarity may mean that the free radicals that are detected at room temperature in these polyimides are predominantly the more stable ones with similar molecular structures involving the imide moiety. Jellinek and Dunkle[20] also pointed out that oxidative degradation during aging at elevated temperatures likely involves production of radicals by rupture of the carbon−nitrogen bond in the imide linkage, because this is the lowest energy bond in the polyimide. When the sample temperature is raised above 300 °C in an oxidative atmosphere, these free radicals undergo degradation, losing fragments with low molar mass. The nearly constant depth of <200 μm for the damaged layer during most of the weight loss indicates that the oxidative degradation process quickly reaches a steady state rate determined by the diffusion rate of the oxygen molecules and the rate of loss of the volatile degradation products from the oxygen-rich surface layer.[11]

Many important solid polymeric materials[6] contain free radicals that can be detected at ambient conditions. Some have free radicals introduced during polymerization and others have free radicals generated when the material is exposed to an elevated temperature during postcuring or aging processes. Because most organic free radicals are reactive species, they are suspected to be responsible for degradation of the polymeric material. When the free radical concentration is high enough, EPRI of such material can provide valuable information concerning the spatial distribution of the free radicals. The EPRI of PMR-15 reported here demonstrates this possibility.

Acknowledgment. This project was, in part, supported by the Indiana State University Research Committee and the NSF.

References and Notes

(1) Meador, M. A.; Cavano, P. J.; Malarik, D. C.; High Temperature Polymer Matrix Composites for Extreme Environments. In *Proceedings of the Sixth Annual ASM/ESD Advanced Composites Conference*, Detroit, Michigan, October 1990; p 529.
(2) Waters, J. F.; Sukenik, C. N.; Kennedy, V. O.; Livneh, M.; Youngs, W. J.; Sutter, J. K.; Meador, M. A. B.; Burke, L. A.; Ahn, M. K. *Macromolecules* **1992**, *25*, 3868.
(3) Ahn, M. K.; Smirnov, A. I.; Smirnova, T. I.; Belford, R. L. *Macromolecules* **1995**, *28*, 7026.
(4) Ahn, M. K.; Stringfellow, T.; Fasano, M.; Bowles, K.; Meador, M. A. *J. Polym. Sci. Part B* **1993**, *31*, 831.
(5) Ahn, M. K.; Stringfellow, T.; Lei, J.; Bowles, K. J.; Meadow, M. A. *MRS Proceedings - High-Performance Polymers* **1993**, *305*, 217.
(6) Ranby, B.; Rabek, J. F. *ESR Spectroscopy in Polymer Research*; Springer-Verlag: Berlin, 1977.
(7) Eaton, G. R.; Eaton, S. S.; Ohno, K. Eds.; *EPR Imaging and Vivo EPR*; CRC: Boca Raton, FL, 1991.
(8) Sueki, M.; Austin, W. R.; Shang, L.; Kerwin, D. B.; Leisure, R. G.; Eaton, G. R.; Eaton, S. S. *J. Appl. Phys.* **1995**, *77*, 790.
(9) (a) Vannucci, R. D.; Alston, W. B. PMR Polyimides with Improved High Temperature Performance. In *Proceedings of the 31st Annual Conference*; Reinforced Plastics/Composite Institute: Washington, DC, 1976; Section 20A, pp 1−8. (b) Johnston, J. C.; Meador, M. A. B.; Alston, W. B. *J. Polym. Sci.: Part A* **1987**, *25*, 2175.
(10) Bowles, K. J.; Jayne D.; Leonhardt, T. A. *SAMPE Quarterly* **1993**, *24*, 2.
(11) (a) Meador, M. A. B.; Lowell, C. E.; Cavano, P. J.; Herrara-Fierro, P. *High Performance Polym.* **1996**, *8*, 363.
(12) Ahn, M. K.; Meador, M. A. B.; Budil, D. E.; Earle, K. A.; Moscicki, J.; Freed, J. H. *Abstracts of Papers*, 17th International EPR Symposium, 36th Rocky Mountain Conference, Denver, August 1994; Abstract 99.
(13) (a) McConnell, H. M. *J. Chem. Phys.* **1956**, *24*, 764; (b) McConnell, H. M.; Chestnut, D. B. *J. Chem. Phys.* **1958**, *28*, 107.
(14) Wertz, J. W.; Bolton, J. R. *Electron Spin Resonance Elementary Theory and Practical Applications*; McGraw-Hill: New York, 1972.
(15) Ahn, M. K.; Weber, R. T.; Meador, M. A. B. In *Proceedings, 6th Annual HITEMP Review: NASA Conference Publication 19117*; Gray, H. R.; Gintry, C. A., Eds.; October 1993; pp 20−21.
(16) Wilson, D. *Br. Polym. J.* **1988**, *20*, 405.
(17) Meador, M. A. B.; Johnston, J. C.; Cavano, P. J. *Macromolecules* **1997**, *30*, 515.
(18) Meador, M. A. B.; Johnston J. C.; Cavano, P. J.; Frimer, A. A. *Macromolecules* **1997**, *30*, 3215.
(19) Hergenrother, P. M. *Angew. Chem., Int. Ed. Engl.* **1990**, *29*, 1262.
(20) Jellinek, H. H. G.; Dunkle, S. R., In *Degradation and Stabilization of Polymers*, Jellinek, H. H. G., Ed.; Elsevier: Amsterdam, 1983; p 66.

MA970580T